International Journal of Thermofluids 18 (2023) 100339

Contents lists available at ScienceDirect

International Journal of Thermofluids

journal homepage: www.sciencedirect.com/journal/international-journal-of-thermofluids

# Numerical solution of Maxwell-Sutterby nanofluid flow inside a stretching sheet with thermal radiation, exponential heat source/sink, and bioconvection

Khalid Abdulkhaliq M. Alharbi [a], Umar Farooq [b,*], Hassan Waqas [c], Muhammad Imran [b,**], Sobia Noreen [d], Ali Akgül [e,f,g], Dumitru Baleanu [h], Sayed M.El Din [i], Khizer Abbas [j]

[a] Mechanical Engineering Department, College of Engineering, Umm Al-Qura University, Makkah 24382, KSA
[b] Department of Mathematics, Government College University Faisalabad, 38000, Pakistan
[c] School of Energy and Power Engineering, Jiangsu University, Zhenjiang 2122013, China
[d] Department of Chemistry, Government College WomenUniversity Faisalabad, 38000, Pakistan
[e] Department of Computer Science and Mathematics, Lebanese American University, Beirut, Lebanon
[f] Siirt University, Art and Science Faculty, Department of Mathematics, 56100 Siirt, Turkey
[g] Near East University, Mathematics Research Center, Department of Mathematics, Near East Boulevard, PC: 99138, Nicosia /Mersin 10–Turkey
[h] Çankaya University, Department of Mathematics, Ankara Turkey
[i] Center of Research, Faculty of Engineering, Future University in Egypt, New Cairo 11835, Egypt
[j] Department of Mathematics and Statistics, University of Agriculture, Faisalabad, 38000, Pakistan

ARTICLE INFO

*Keywords:*
Maxwell-Sutterby nanofluid
Exponential heat source/sink
Thermal radiation
Activation energy
Motile microorganisms
Bioconvection
Stretching sheet
Shooting approach

ABSTRACT

A Survey of literature illustrates that nano liquid is further helpful for heat transportation as compared to regular liquid. Nonetheless, there are considerable gaps in our understanding of existing approaches for enhancing heat transmission in nanofluids, necessitating comprehensive research of these fluids. The current approach proposes to investigate the influence of a Maxwell-Sutterby nanofluid on a sheet while accounting for heat radiation. This paper investigates activation energy, and exponential heat source/sink. Bioconvection and motile microorganisms with Brownian motion and thermophoresis effects are considered.y linked similarity transformations, the boundary layer set of controlling partial differential equations are transformed into ordinary differential equations. A numerical strategy (shooting technique) is used to handle the transformed system of ordinary differential equations through the Bvp4c solver of the computing tool MATLAB. The results for velocity and temperature, concentration, and motile microbe profiles are numerically and graphically examined for various parameters. The velocity distribution profile decreased as the magnetic parameter varied, but increased when the mixed convection parameter increased in magnitude. The heat flux profile is improved with higher estimations of the Biot number and thermophoresis parameter. When the Prandtl number and the Brownian motion parameter's values rise, the energy profile falls. When the Peclet number and bioconvection Lewis number increased, the profile of mobile microorganisms dropped.

## 1. Introduction

Recent applications of nanomaterials have allowed the development of a new form of fluid called nano-liquid. The dilute aggregation of nanoparticles immersed in a low thermal conductivity base liquid has aroused the interest of researchers. The base liquid, or displacement medium, may be aqueous or non-aqueous in design. Typical nanomaterials are metallic oxides, carbon steels, and alloys these objects can be powder, cylindrical, spherical, tubes, etc.By employing entities substances, the heat transfer rate is raised, which increases the usefulness of base fluids. Several of these fluids are classified as non-Newtonian fluids of varying composition from Newtonian fluids. It is usually accepted that non-Newtonian fluids displaying a nonlinear connection through strain rate are much more suitable for industrial

* Corresponding author.
** Corresponding author.
*E-mail addresses:* umar_farooq@gcuf.edu.pk (U. Farooq), drmimranchaudhry@gcuf.edu.pk (M. Imran).

https://doi.org/10.1016/j.ijft.2023.100339

Available online 22 March 2023

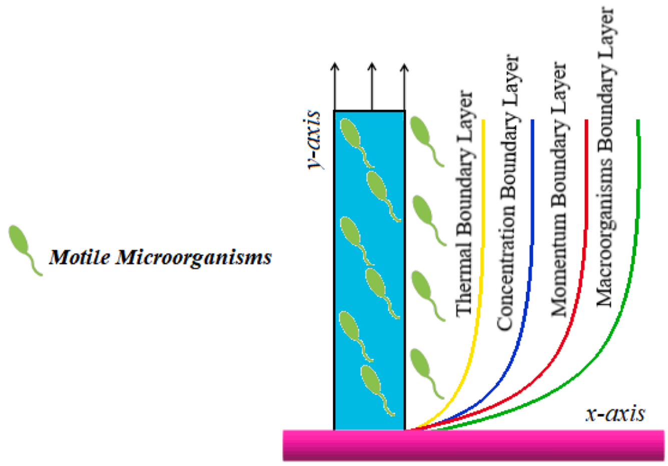


**Fig. 1.** Configuration of flow problem.

uses than Fluids with Newtonian properties. Non-Newtonian fluid examples include drug items, beauty products, paints, manufacturing lubricants, body tissues packaged foods, etc.Nearly all scientific disciplines, including inorganic chemistry, cardiology, thermal spray physics, astronomy, physical geology, and others, heavily rely on heat transmission. As a result, several studies in the literature have taken into account heat transmission across various fluid fluxes. Several engineering procedures, such as liquid metal purification, heat exchanger, controlled nuclear cooling, etc., are the applications of the analysis of heat transfer.Choi [1] looked into the topic of nanofluids. Buongiorno [2] discussed Movement and heat transfer by convection in nanofluids. Hsiao [3] talked about the importance of a magnetic field in mixed convection. Rashidi et al. [4] studied the properties of nano liquid over a stretched sheet using a non-linear thermal radiation method. Sheikholeslami and Bhatti [5] demonstrated the significance of nano-liquid flow with gravitational tension and forced convection. Turkyilmazoglu [6] investigated the influences of nanofluid flow through a curved vertical wall. Using heat radiation and MHD, Ellahi et al. [7] deduced the relevance of Jeffrey nanofluid between two discs. The Mixed convection flow hypothesis and the Bioconvectional flow of nanofluid with heat radiation across a cylinder were found by Farooq et al. [8]. Rashid et al. looked into the properties of Maxwell nanofluids in the presence of hot radiation and MHD flow. [9].Thermal radiation refers to the emission of electromagnetic waves from the surface of an object due to its temperature. All objects with a temperature above absolute zero emit thermal radiation. This radiation can include infrared radiation, visible light, ultraviolet radiation, and even radio waves. The amount and spectrum of thermal radiation emitted by an object depend on its temperature and the material properties of its surface. As the temperature of an object increases, the amount of thermal radiation it emits also increases, and the wavelengths of the emitted radiation become shorter. This is why hot objects glow red, yellow, or white, depending on their temperature. Tayebi et al. investigated the magnetized fluid mechanics and heat radiation effects of a hybrid nanofluid. [10]. Hayat et al. investigated the usage of chemical potential and heating effect in the MHD boundary layer flow of nanofluid. [11]. Muhammad et al. [12] showed the three-dimensional flow of activated nanofluid across a Riga plate. Alamri et al. [13] employed nanofluid to study the effects of second-order sliding across a porous media. Khan et al. [14] looked at the effects of stratification and heat generation characteristics of Prandtl fluid with mixed convection flows through a porous medium. Using MHD across a disc, Anwar et al. [15] examined the effects of non-linear radiative heat transmission. On a Riga surface, Gailitis and Lielausis [16] created a nanofluid with the MHD effect. Riaz et al. [17] investigated the heat transmission of a nanofluid across a curved porous conduit. Waqas et al. [18] looked into the impact of an Eyring-Powell nanofluid with a permanent magnet field and activation energy. A radiative nanofluid including nanoparticles was studied by Farooq et al. [19] for its effects on a surface.A cylinder or plate was the subject of research by Farooq et al. [20] into heat transmission, bioconvection, and motile microorganisms in a Casson nanofluid. With the use of the CattaneoChristov model and heat radiation across a narrow cylinder, Farooq et al. [21]. simulation of Williamson nanofluid flow. Khan [22] used bioconvection and nanofluid flow to explore microorganisms. The impact of natural convection flow on the flow of a stretched sheet of Casson nanofluid was investigated by Humane et al. [23]. The bioconvective flow of a Jeffrey nanofluid with inconstant fluid characteristics and radiation was investigated by Hussein et al. [24]. In their work, Iqbal et al. [25] investigated the role of bio convectional over Powell-Eyring nanofluid with heat radiation.Haq et al. [26] looked into the impacts of nanofluid flow through some kind of wedge with thermal conduction and porous material. The effects of boundary layer flow accidental convection flow over a tube were investigated by Ali et al. [27]. Qasem et al. [28] studied the effect of nanoparticles on the creation of heat and entropy across a cylinder. Abbassi et al. [29] studied the effects of base fluid on a heating block with free convection. Abbassi et al. [30] used LBM simulated and a heated block to study the significance of nanoparticles.

Bioconvection is the active free motion of a large number of microscopic microorganisms in a fluid. Chemotaxis, oxytactic, gyrotactic, and negative gravitaxis are the three types of moving microorganisms. Bioconvection is important in applications such as biofuels, ethanol, and environmentally friendly industrial operations. Apart from that, buoyant forces, microbes, and nanoparticles are used to create nanoparticle bioconvection. Due to the possibility that motile bacteria may effectively attain nanoparticle stability within the base fluid, convective heat transfer has gained a lot of attention lately. Kuznetsov [31] investigated the impact of bioconvection on microorganisms. Second-grade nanofluids were studied by Li et al. [32] about their function in bioconvection and heat radiation. Muhammad et al. [33] studied the influence of mixed convection flow on the Carreau nanofluids over a wedge. The skin friction flow of a pair of stress nanofluids in the absence of consists of cellulose and motile microorganisms was explored by Khan et al. [34]. Zhang et al. [35] employed shrinking discs to evaluate the properties of nanofluid and bioconvection. Waqas et al. [36] investigated Oldroyd-B fluid flow with convective heat across a rotating disc. Khan et al. [37] investigated the effects of bioconvection on double discs using entropy and the Buongiorno approach. Mamatha et al. [38] investigated the influence of MHD on nanofluid flow towards the centreline across a sheet. Ferdows et al. [39] investigated cylinder-based mass and heat transmission. The effects of moving microorganisms flowing in three dimensions in bioconvection and nanofluid were investigated by Amirsom et al. [40]. The impact of solid surface tension on the recognition of nanotechnology-enhanced biomaterial structures was examined by Kasaragadda et al. [41]. The interactions of Casson liquid and bioconvection flow with motile microorganisms were studied by Ansari et al. [42].

The current study's primary goal is to examine the importance of a Maxwell-Sutterby nanofluid via a sheet with thermal conductivity, both bioconvection and movable microbes. Effects of thermophoresis and Brownian motion are also researched. By tackling exponential heat source and sink, as well as the thermal conductivity impact with convective boundary conditions, the study achieves novelty; such a physical scenario has not before been addressed in the literature. The primary governing PDEs are translated into ordinary differential equations using similarity transformations in the computer software MATLAB using the built-in function bvp4c. To verify the outcomes and uncover good agreement, a comparison research was undertaken between published work and current results.

## 2. Mathematical formulations

We looked at the Maxwell-Sutterby nanofluid flow in two dimensions

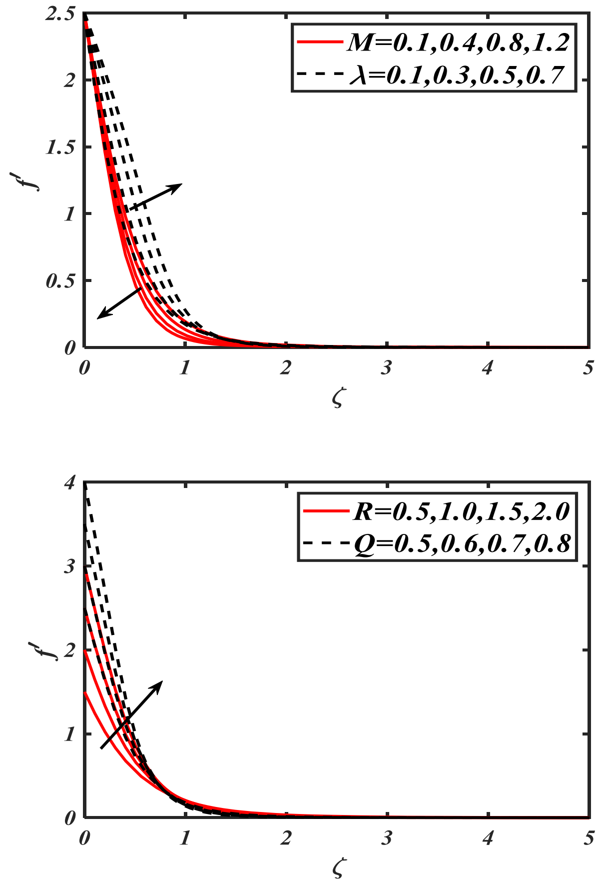


**Fig. 2.** (a): Deviation of velocity distribution $f$ for $M\&\lambda$ (b): Deviation of velocity distribution $f$ for $R\&Q$.

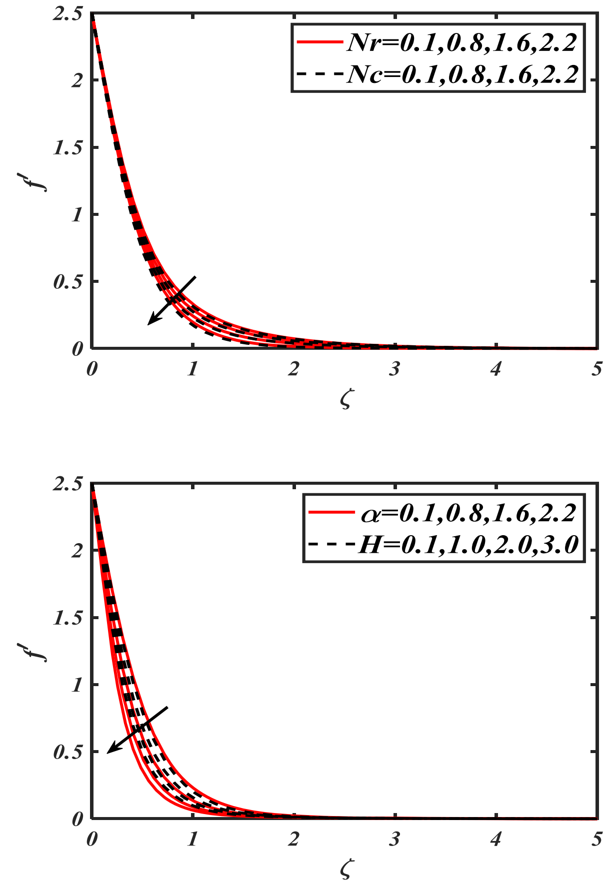


**Fig. 3.** (a): Deviation of velocity distribution $f$ for $Nr\&Nc$ (b): Deviation of velocity distribution $f$ for $\alpha\&H$.

across a stretched sheet of motile microorganisms and bioconvection. The impacts of radiant heat, exponential heat source/sink, and kinetic energy are explored. The effects of Brown's law and thermophoresis are studied. The sheet is positioned vertically and has separate velocities in the axis as illustrated in Fig. 1.

The following are the major assumptions of the current flow problem:

- The two-dimensional flow of Maxwell-Sutterby nanofluid across a stretched sheet.
- Thermal energy with an exponential heat source/sink is investigated.
- The impact of activation energy and MHD is also examined.
- Bioconvection and motile microorganisms are also researched.

The following are the main equations [43]:

***Continuity equation***

$$u_x + v_y = 0, \tag{1}$$

***Momentum equation***

$$uu_x+vv_y+\lambda_1\left(u^2u_{xx}+v^2+2uvu_{xy}\right)=\frac{\nu}{2}u_{yy}\left[1-\frac{mb^2}{2}\left(v_y\right)^2\right]-\frac{\sigma B_0^2}{\rho}\left(u+\lambda_1 vu_y\right)$$
$$+\frac{1}{\rho_f}\left[\left(1-C_f\right)\rho_f\beta^{**}g^*\left(T-T_\infty\right)-\left(N-N_\infty\right)\left(\rho_p-\rho_f\right)g^*-\left(C-C_\infty\right)g^*\gamma\left(\rho_m-\rho_f\right)\right], \tag{2}$$

**Energy equation**

$$uT_x + vT_y = \frac{1}{\rho c_p}\partial_y\left(kT_y\right) + \frac{(\rho c_p)_p}{(\rho c_p)_f}\left\{D_B\frac{\partial T}{\partial y}\frac{\partial C}{\partial y} + \frac{D_T}{T_\infty}\left(\frac{\partial T}{\partial y}\right)^2\right\} + \frac{Q_T^*}{\rho C_p}(T-T_\infty)$$
$$+\frac{Q_E^*}{\rho C_p}(T_w - T_\infty)e^{-\sqrt{(b/\nu_f)}ny}, \tag{3}$$

***Concentration equation***

$$uC_x + vC_y = \partial_y\left[D(C)C_y\right] + D_B\partial_y C_y + \frac{D_T}{T_\infty}\partial_y T_y$$
$$- Kr^2(C - C_\infty)\left(\frac{T}{T_\infty}\right)^m \exp\left(\frac{-E_a}{kT}\right), \tag{4}$$

***Microorganism's equation***

$$uN_x + vN_y + \frac{bW_c}{(C_w - C_\infty)}\left[\partial_y\left(NC_y\right)\right] = D_m N_{yy}, \tag{5}$$

***Boundary conditions***

$$\left.\begin{array}{lll} y=0, \mu u_y|_{y=0} = \sigma_x|_{y=0} = \sigma_T T_x|_{y=0} - \sigma_C C_x|_{y=0}, & & \\ v=0, -kT_y = h_f(T_w - T), D_B C_y + \frac{D_T}{T_\infty}T_y = 0, N = N_w & & \\ at\ \ r=R, & y\to\infty, & u=0, \\ T\to T_\infty, & C\to C_\infty, & N\to N_\infty \end{array}\right\}. \tag{6}$$

The term for non-uniform thermal conductivity and concentration diffusivity is:

$$k = k_\infty(1 + \in_1\theta), \tag{7}$$

The variable molecular diffusivity

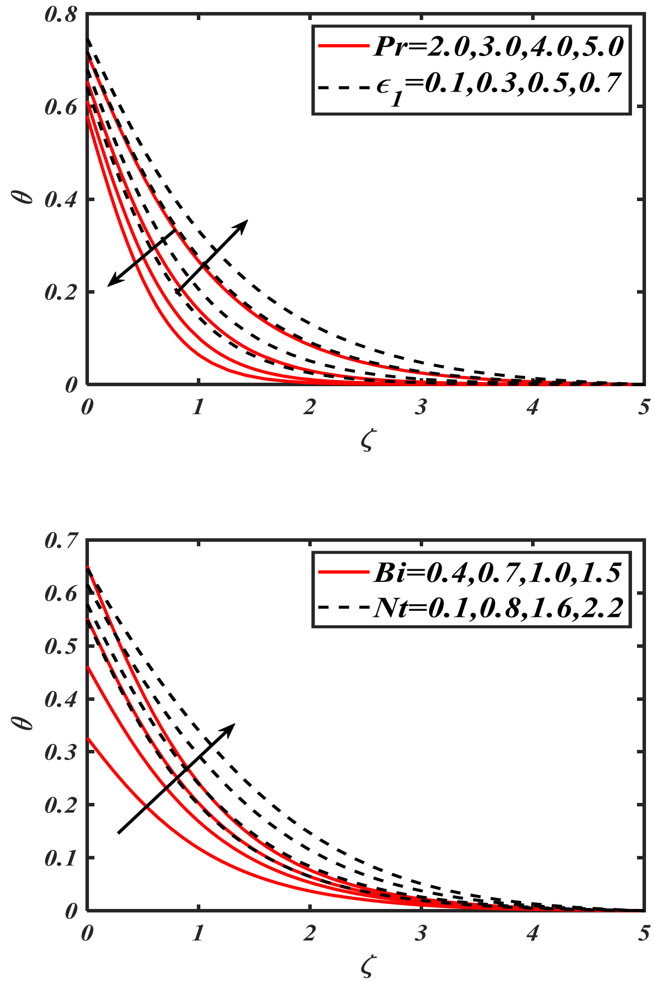


**Fig. 4.** (a): Deviation of temperature distribution onPr&$\in_1$ (b): Deviation of temperature distribution for*Bi*&*Nt*.

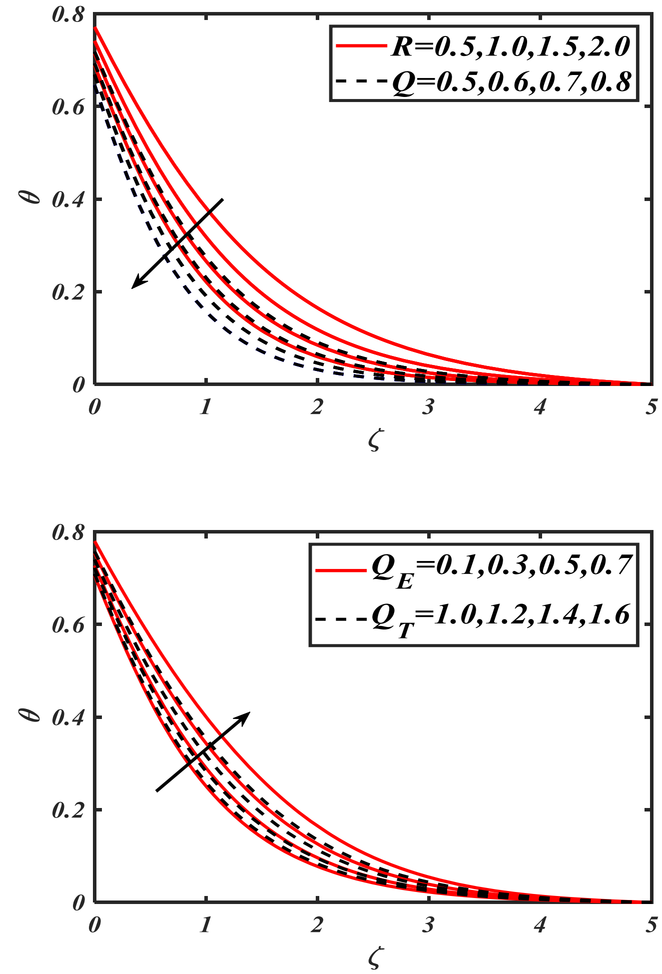


**Fig. 5.** (a): Deviation of temperature distribution for*R*&*Q*. (b): Deviation of temperature distribution θ for $Q_E$&$Q_T$.

$$D_B = D_{B\infty}(1 + \in_2 \phi), \tag{8}$$

Furthermore, the surface tension $\sigma$ is related linearly to concentration and temperature:

$\sigma = \sigma_0 - \gamma_\tau(T - T_\infty) - \gamma_c(C - C_\infty)$, The symbols $\sigma_0,\gamma_\tau\gamma_c$ are positive constants $\sigma_\tau = \sigma_T|_{T=T_\infty}$, $\sigma_c = \sigma_C|_{C=C_\infty}$

With appropriate similarity transformation [43]

$$\left.\begin{array}{l} u\left[= axf'(\zeta)\right], \quad v\left[= -\sqrt{a\nu}f(\zeta)\right], \quad \zeta\left[= \sqrt{\frac{a}{\nu}}y\right], \\ \theta(\zeta)\left[= \frac{T - T_\infty}{T_w - T_\infty}\right], \phi(\zeta)\left[= \frac{C - C_\infty}{C_w - C_\infty}\right], \chi(\zeta)\left[= \frac{N - N_\infty}{N_w - N_\infty}\right]. \end{array}\right\}, \tag{9}$$

Invoking suitable similarity transformation (9), Eq. (1) is easily checked, and expresses (2–5) are transformed to following

$$\left[\left(1 - \frac{m}{2}\mathrm{ReH}f''^2\right) - 2\alpha f^2\right]f''' + 4\alpha ff'f'' - 2Mf' + 2M\alpha ff'' - 2f'^2 + 2ff'' + \lambda(\theta - Nr\phi - Nc\chi) = 0, \tag{10}$$

$$(1 + \in_1\theta)\theta'' + \in_1\theta'^2 + \mathrm{Pr}f\theta' + \mathrm{Pr}Nb\phi'\theta' + \mathrm{Pr}Nt\theta'^2 + \mathrm{Pr}Q_T\theta + \mathrm{Pr}Q_Ee^{-n\zeta} = 0, \tag{11}$$

$$(1 + \in_2\phi)\phi'' + \in_2\phi'^2 + fLe\mathrm{Pr}\phi' + \frac{Nt}{Nb}\theta'' + \sigma Le\mathrm{Pr}(1 + \delta\theta)^m\exp\left(\frac{-E}{1 + \delta\theta}\right)\phi = 0, \tag{12}$$

$$\chi'' + Lb\chi'f - Pe[\phi''(\chi + \delta) + \chi'\phi'] = 0, \tag{13}$$

With restrictive conditions (6) as transformed

$$\left.\begin{array}{c} \zeta = 0, \quad f(\zeta) = 0, \quad f''(\zeta)|_{\zeta=0} = -1Q(1 + R) \\ \theta'(0) = -Bi(1 - \theta(0)), \quad \theta(\infty)\to 0, \\ Nb\phi' + Nt\theta' = 0, \quad \phi(\infty)\to 0, \quad \chi'(0) = 1, \quad \chi(\infty)\to 0, \\ \zeta\to\infty, \quad f'(\zeta)\to\infty, \quad \theta(\zeta)\to\infty, \quad \phi(\zeta)\to\infty, \quad \chi(\zeta)\to\infty. \end{array}\right\}, \tag{14}$$

The flow parameters are listed here:

| Maxwell fluid Deborah's number | $\alpha(=\lambda_1 a)$ |
|---|---|
| Activation energy parameter | $E\left(=\frac{E_a}{kT_\infty}\right)$ |
| Temperature difference parameter | $\delta\left(=\frac{T_w - T_\infty}{T_\infty}\right)$ |
| Reynolds number | $\mathrm{Re}\left(=\frac{ax^2}{\nu}\right)$ |
| Sutterby fluid Deborah's number | $H\left(=\frac{b^2a^2}{\nu}\right)$ |
| Magnetic parameter | $M\left(=\frac{\sigma B_0^2}{\rho a}\right)$ |
| Lewis number | $Le\left(=\frac{\alpha}{D_{B_\infty}}\right)$ |
| Heat source parameter | $Q_T\left(=\frac{Q_T^*}{\rho C_p a}\right)$ |
| Heat sink parameter | $Q_E\left(=\frac{Q_E^*}{\rho C_p a}\right)$ |

(*continued on next page*)

(*continued*)

| Maxwell fluid Deborah's number | $\alpha(=\lambda_1 a)$ |
|---|---|
| Prandtl number | $\Pr\left(=\frac{\nu}{\alpha}\right)$ |
| Mixed convection parameter | $\lambda\left(=\frac{\beta^{**}g*(1-C_\infty)(T_w-T_\infty)}{aU_w}\right)$ |
| Buoyancy ratio parameter | $Nr\left(=\frac{(\rho_p-\rho_f)(C_w-C_\infty)}{\rho_f(1-C_\infty)(T_w-T_\infty)\beta^{**}}\right)$ |
| Bioconvection Rayleigh number | $Nc\left(=\frac{\gamma*(\rho_m-\rho_f)(N_w-N_\infty)}{\rho_f(1-C_\infty)(T_w-T_\infty)\beta^{**}}\right)$ |
| Brownian motion parameter | $Nb\left(=\frac{\tau D_B(C_w-C_\infty)}{\nu}\right)$ |
| Thermophoresis parameter | $Nt\left(=\frac{\tau D_T(T_w-T_\infty)}{\nu T_\infty}\right)$ |
| Peclet number | $Pe\left(=\frac{bW_c}{D_m}\right)$ |
| Bioconvection Lewis number | $Lb\left(=\frac{\nu}{D_m}\right)$ |
| Marangoni number | $Q\left(=\frac{\gamma_T A}{\mu\Omega}\sqrt{\frac{\Omega}{\gamma}}\right)$ |
| Marangoni ratio parameter | $R\left(=\frac{\gamma_C B}{\gamma_T A}\right)$ |
| Biot number | $Bi\left(=\frac{h_f}{k}\sqrt{\frac{\nu}{a}}\right)$ |

The engineering quantities are defined as:

$$Cf_x\left(=\frac{\tau_w}{\rho U_w^2}\right), Nu_x\left(=\frac{xq_w}{k(T_w-T_\infty)}\right), Sh_x\left(=\frac{xq_m}{k(C_w-C_\infty)}\right), \quad (15)$$

Where

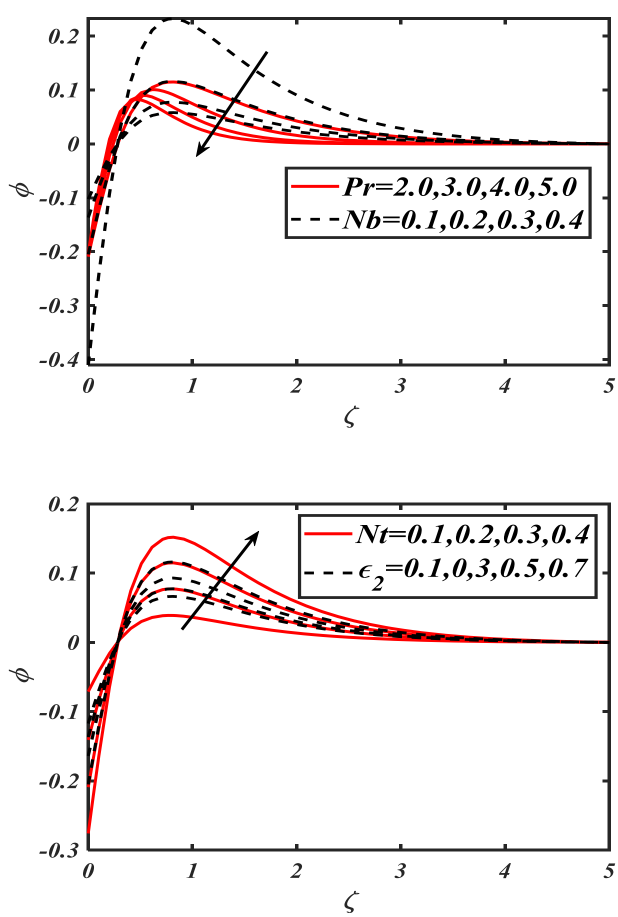


**Fig. 6.** (a): Deviation of volumetric distribution ϕ for Pr&$Nb$. (b): Deviation of volumetric distribution ϕfor $Nt$&$\in_2$.

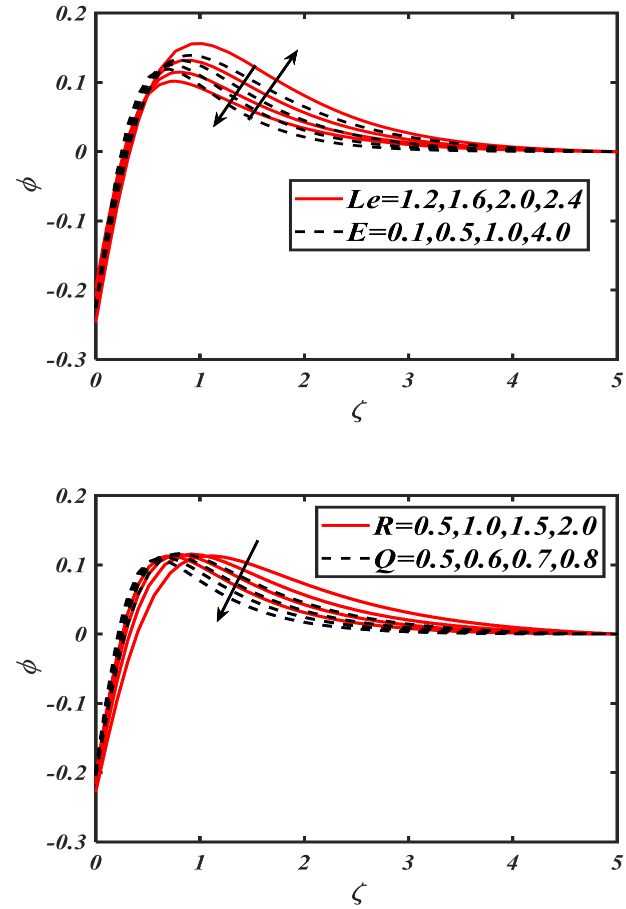


**Fig. 7.** (a): Deviation of volumetric distribution for$Le$&$E$. (b): Deviation of volumetric distribution $R$&$Q$.

$$\tau_w=-\mu\left[(1+\alpha)u_y+\frac{mb^2}{3}(u_y)^3\right] \quad (16)$$

$$q_w=-kT_y, q_m=-D_B(C_y) \quad (17)$$

Following is the dimensionless form of physical quantities of interest:

$$Cf_x\mathrm{Re}_x^{-\frac{1}{2}}=-\left[(1+\alpha)f''+\frac{m}{3}\mathrm{ReH}f''^3\right], \quad (18)$$

$$Nu_x\mathrm{Re}_x^{-\frac{1}{2}}=-\theta'(0), \quad (19)$$

$$Sh_x\mathrm{Re}_x^{-\frac{1}{2}}=-\phi'(0), \quad (20)$$

## 3. Numerical scheme

Using the built-in MATLAB function bvp4c [44–46] and a shooting method, the nonlinear non-dimensional transformed governing problem Eqs. (10–13) and boundary conditions (14) were solved. Until the solution reaches the requisite accuracy, the shooting strategy is used to integrate first-order ODEs with starting conditions, and any missing initial conditions are replaced using Newton's technique. To get numerical and graphical findings for the current issue, we used the MATLAB/Simulink tool. The numerical results of this issue are all subject to an error tolerance $10^{-6}$. The PDE system is transformed into first-order ODEs by employing the variables.

Let,

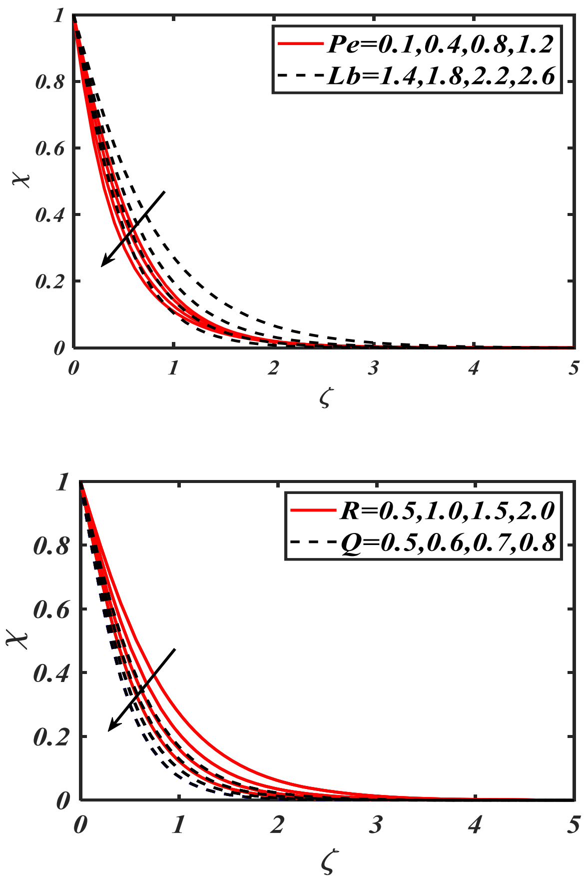


**Fig. 8.** (a): Deviation of motile microorganisms' profile$\chi$*Pe&Lb*. (b): Deviation of motile microorganisms' profile$\chi$for *R&Q*.

$$\left.\begin{array}{llll} f = h_1, & f' = h_2, & f'' = h_3, & f''' = h'_3, \\ \theta = h_4, & \theta' = h_5, & \theta'' = h'_5, & \\ \phi = h_6, & \phi' = h_7, & \phi'' = h'_7, & \\ \chi = h_8, & \chi' = h_9, & \chi'' = h'_9 & \end{array}\right\}, \tag{21}$$

$$h'_3 = \left.\frac{2Mh_2 - 2M\alpha h_1 h_3 + 2{h_2}^2 - 2h_1 h_3 - \lambda(h_4 - Nrh_6 - Nch_8)}{\left(\left(1 - \frac{m}{2}\mathrm{ReH}{h_3}^2\right) - 2\alpha {h_1}^2 + 4\alpha h_1 h_2\right)}\right\}, \tag{22}$$

$$h'_5 = \left.\frac{-\in_1 h_5^2 - \mathrm{Pr} h_1 h_5 - \mathrm{Pr} Q_T h_4 - \mathrm{Pr} Q_E e^{-n\zeta}}{(1 + \in_1 h_4)}\right\}, \tag{23}$$

$$h'_7 = \left.\frac{-\in_2 {h_7}^2 - Le\mathrm{Pr} h_1 h_7 - \sigma Le\mathrm{Pr}(1 + \delta h_4)^m \exp\left(\frac{-E}{1+\delta h_4}\right) h_6}{(1 + \in_2 h_6)}\right\}, \tag{24}$$

$$h'_9 = -Lbh_9 h_1 + Pe[h'_7(h_8 + \delta) + h_9 h_7]\}, \tag{25}$$

With

$$\left.\begin{array}{l} \zeta = 0, \quad h_1(\zeta) = 0, \quad \left(1 + \frac{1}{\beta}\right) h_2(\zeta)|_{\zeta=0} = -1Q(1+R), \\ h_5(0) = -Bi(1 - h_4(0)), \quad h_4(\infty) \to 0, \\ Nbh_7 + Nth_5 = 0, \quad h_6(\infty) \to 0, \quad h_9(0) = 1, \quad h_8(\infty) \to 0, \\ \zeta \to \infty, \quad h_2(\zeta) \to \infty, \quad h_4(\zeta) \to \infty, \quad h_6(\zeta) \to \infty, \quad h_8(\zeta) \to \infty. \end{array}\right\}. \tag{26}$$

## 4. Results and discussion

In this part, using profiles of motile microorganisms, temperature, concentration, and velocity, we examine the effects of flow factors. The effects of physical flow parameters such as the Schmidt number, the mixed convection parameter, the Marangoni number, the Marangoni ratio variable, the Sutterby fluid Deborah quantity, the Maxwell fluid Deborah number, the bioconvection Rayleigh number, the buoyancy ratio component, the thermal conductivity parameter, the Local nusselt number, the Biot multitude, the thermal radiation, the Brownian motion parameter, the free convection Peclet number Figs. 2 (a, b)–8 (a, b).

**Table 1**
The difference in $-\theta'(0)$physical flow parameters.

| *M* | λ | *Nr* | *Nc* | *Q* | Pr | *Nb* | *Nt* | *Bi* | *R* | $-\theta'(0)$ |
|---|---|---|---|---|---|---|---|---|---|---|
| 0.2 | 0.2 | 0.1 | 0.1 | 0.5 | 2.0 | 0.2 | 0.3 | 1.0 | 0.2 | **0.4607** |
| 0.6 | | | | | | | | | | **0.4532** |
| 1.2 | | | | | | | | | | **0.4428** |
| 0.1 | **0.1** | 0.1 | 0.1 | 0.5 | 2.0 | 0.2 | 0.3 | 1.0 | 0.2 | **0.4621** |
| | **0.6** | | | | | | | | | **0.4647** |
| | **1.2** | | | | | | | | | **0.4677** |
| 0.1 | 0.2 | **0.2** | 0.1 | 0.5 | 2.0 | 0.2 | 0.3 | 1.0 | 0.2 | **0.4626** |
| | | **0.8** | | | | | | | | **0.4615** |
| | | **1.6** | | | | | | | | **0.4578** |
| 0.1 | 0.2 | 0.1 | **0.2** | 0.5 | 2.0 | 0.2 | 0.3 | 1.0 | 0.2 | **0.4624** |
| | | | **0.8** | | | | | | | **0.4613** |
| | | | **1.6** | | | | | | | **0.4597** |
| 0.1 | 0.2 | 0.1 | 0.1 | **0.1** | 2.0 | 0.2 | 0.3 | 1.0 | 0.2 | **0.4851** |
| | | | | **0.4** | | | | | | **0.5123** |
| | | | | **0.8** | | | | | | **0.5522** |
| 0.1 | 0.2 | 0.1 | 0.1 | 0.5 | **1.0** | 0.2 | 0.3 | 1.0 | 0.2 | **0.3474** |
| | | | | | **3.0** | | | | | **0.5313** |
| | | | | | **5.0** | | | | | **0.6097** |
| 0.1 | 0.2 | 0.1 | 0.1 | 0.5 | 2.0 | **0.1** | 0.3 | 1.0 | 0.2 | **0.4626** |
| | | | | | | **0.4** | | | | **0.4658** |
| | | | | | | **0.7** | | | | **0.4699** |
| 0.1 | 0.2 | 0.1 | 0.1 | 0.5 | 2.0 | 0.2 | **0.1** | 1.0 | 0.2 | **0.4702** |
| | | | | | | | **0.4** | | | **0.4587** |
| | | | | | | | **0.8** | | | **0.4467** |
| 0.1 | 0.2 | 0.1 | 0.1 | 0.5 | 2.0 | 0.2 | 0.3 | **0.2** | 0.2 | **0.1623** |
| | | | | | | | | **0.8** | | **0.4010** |
| | | | | | | | | **1.4** | | **0.5006** |

**Table 2**
The difference $-\phi'(0)$in physical flow parameters.

| $M$ | $\lambda$ | $Nr$ | $Nc$ | $Q$ | Pr | $Nb$ | $Nt$ | $Le$ | $R$ | $-\phi'(0)$ |
|---|---|---|---|---|---|---|---|---|---|---|
| 0.2 | 0.2 | 0.1 | 0.1 | 0.5 | 2.0 | 0.2 | 0.3 | 2.0 | 0.2 | **0.6910** |
| 0.6 | | | | | | | | | | **0.6797** |
| 1.2 | | | | | | | | | | **0.6642** |
| 0.1 | **0.1** | 0.1 | 0.1 | 0.5 | 2.0 | 0.2 | 0.3 | 2.0 | 0.2 | **0.6931** |
| | **0.6** | | | | | | | | | **0.6971** |
| | **1.2** | | | | | | | | | **0.7015** |
| 0.1 | 0.2 | **0.2** | 0.1 | 0.5 | 2.0 | 0.2 | 0.3 | 2.0 | 0.2 | **0.6939** |
| | | **0.8** | | | | | | | | **0.6914** |
| | | **1.6** | | | | | | | | **0.6897** |
| 0.1 | 0.2 | 0.1 | **0.2** | 0.5 | 2.0 | 0.2 | 0.3 | 2.0 | 0.2 | **0.6877** |
| | | | **0.8** | | | | | | | **0.7122** |
| | | | **1.6** | | | | | | | **0.7445** |
| 0.1 | 0.2 | 0.1 | 0.1 | **0.1** | 2.0 | 0.2 | 0.3 | 2.0 | 0.2 | **0.7049** |
| | | | | **0.4** | | | | | | **0.6939** |
| | | | | **0.8** | | | | | | **0.6811** |
| 0.1 | 0.2 | 0.1 | 0.1 | 0.5 | **1.0** | 0.2 | 0.3 | 2.0 | 0.2 | **0.5211** |
| | | | | | **3.0** | | | | | **0.7970** |
| | | | | | **5.0** | | | | | **0.9146** |
| 0.1 | 0.2 | 0.1 | 0.1 | 0.5 | 2.0 | **0.1** | 0.3 | 2.0 | 0.2 | **1.3879** |
| | | | | | | **0.4** | | | | **1.3893** |
| | | | | | | **0.7** | | | | **1.3907** |
| 0.1 | 0.2 | 0.1 | 0.1 | 0.5 | 2.0 | 0.2 | **0.1** | 2.0 | 0.2 | **0.2351** |
| | | | | | | | **0.4** | | | **0.2313** |
| | | | | | | | **0.8** | | | **0.2269** |
| 0.1 | 0.2 | 0.1 | 0.1 | 0.5 | 2.0 | 0.2 | 0.3 | **0.2** | 0.2 | **0.7374** |
| | | | | | | | | **0.8** | | **0.7325** |
| | | | | | | | | **1.4** | | **0.7297** |

**Table 3**
The difference $-\chi'(0)$in physical flow parameters.

| $M$ | $\lambda$ | $Nr$ | $Nc$ | $Q$ | $Pe$ | $Lb$ | $-\chi'(0)$ |
|---|---|---|---|---|---|---|---|
| 0.2 | 0.2 | 0.1 | 0.1 | 0.5 | 0.1 | 2.0 | **1.4118** |
| 0.6 | | | | | | | **1.3823** |
| 1.2 | | | | | | | **1.3417** |
| 0.1 | **0.1** | 0.1 | 0.1 | 0.5 | 0.1 | 2.0 | **1.4177** |
| | **0.6** | | | | | | **1.4265** |
| | **1.2** | | | | | | **1.4364** |
| 0.1 | 0.2 | **0.2** | 0.1 | 0.5 | 0.1 | 2.0 | **1.4195** |
| | | **0.8** | | | | | **1.4199** |
| | | **1.6** | | | | | **1.4204** |
| 0.1 | 0.2 | 0.1 | **0.2** | 0.5 | 0.1 | 2.0 | **1.4188** |
| | | | **0.8** | | | | **1.4144** |
| | | | **1.6** | | | | **1.4086** |
| 0.1 | 0.2 | 0.1 | 0.1 | **0.1** | 0.1 | 2.0 | **1.4145** |
| | | | | **0.4** | | | **1.3989** |
| | | | | **0.8** | | | **1.3878** |
| 0.1 | 0.2 | 0.1 | 0.1 | 0.5 | **0.2** | 2.0 | **1.0318** |
| | | | | | **0.6** | | **1.2661** |
| | | | | | **1.2** | | **1.6568** |
| 0.1 | 0.2 | 0.1 | 0.1 | 0.5 | 0.1 | **1.0** | **0.6364** |
| | | | | | | **1.6** | **0.8354** |
| | | | | | | **2.8** | **1.0862** |

**Table 4**
Analysis of the collected results in comparison to Sajid, Ibrahim, and Negara.

| $M$ | Ibrahim and Negera [47] | Sajid et al. [43] | Current outcomes |
|---|---|---|---|
| 0.0 | 1.2106 | 1.2105 | 1.2107 |
| 0.3 | 1.3578 | 1.3394 | 1.3395 |
| 0.5 | 1.4479 | 1.4407 | 1.4408 |
| 1.0 | 1.6505 | 1.6678 | 1.6679 |

Fig. 2 represents the consequences of the magnetic parameter $M$ and mixed convection parameter$\lambda$on the velocity field$f'$. The velocity field decreases as the values of the magnetic parameter grow, but the velocity field increases as the valuations of the assorted convection parameter increase. The very reason lies in the fall that the magnetic parameter is significantly associated with Lorentz force, increasing the values $M$induces more resistance and thus reduces the velocity. In terms of the physical principle, the magnetic field produces a protected force that acts in differing ways of the fluid. Fig. 2b illustrates how the Marangoni number$Q$ and Marangoni ratio parameters$R$ behave on the velocity field$f'$. The Marangoni number and Marangoni ratio parameters are increased by increasing the velocity field$f'$. The effects of the bioconvection Rayleigh number and buoyancy ratio parameter versus the velocity field are shown in Fig. 3a. With rising bioconvection Rayleigh number$Nc$ and buoyancy ratio values$Nr$, the flow velocity profile declines. The effects of the Sutterby fluid Deborah number$\alpha$ and the Maxwell fluid Deborah number$H$ on the velocity field$f'$ are examined in Fig. 3b. The velocity decreased due to the buoyancy proportion and bioconvection Rayleigh number's improved performance. Fig. 4a plots the results of the Prandtl quantityPr and thermal conductivity limit $\in_1$ versus the temperature field$\theta$. As estimates of the thermal conductivity restriction were raised, the temperature field grew while it decreased when the Prandtl number was raised. Because thermal diffusivity and the Prandtl number are opposed, the cooling in the boundary layer domain is apparent. As estimates of the thermal conductivity parameter were raised, the temperature field grew while it decreased when the Prandtl number was raised. Because thermal diffusivity and the Prandtl number are opposed, the cooling in the boundary layer domain is apparent. The impacts of the thermophoresis parameter$Nt$and Biot number$Bi$are depicted by a temperature distribution profile$\theta$ in Fig. 4b. This shows that the flow of the temperature field increases as a result of amplifying fluctuations in the Biot amount$Bi$ and thermophoresis constraint$Nt$. Fig. 5a shows the investigation of the Marangoni number$Q$ and Marangoni ratio parameter$R$ for the temperature field. For the booming variations of the Marangoni number$Q$ and Marangoni ratio parameter$R$, the temperature field is reduced. Fig. 5b considers the effects of the heat base stricture and the exponential heat sink parameter $Q_E$on the temperature field. The temperature distribution has improved due to the exponential heat sink constraint and the heat base parameter's$Q_T$ increasing variation. Fig. 6a illustrates how the Brownian motion parameter$Nb$ and Prandtl numberPr have an impact on the concentration distribution field$\phi$. The concentration of nanoparticles rose as estimates of the Brownian motion parameter and Prandtl number increased. Fig. 6b shows the effects of the concentration conductivity $\in_2$

and thermophoresis parameters$Nt$ on the energy profile. The concentration profile grew when the concentration conductivity $\in_2$ and thermophoresis parameters$Nt$ were valued more intensely. Lewis number and activation energy concentration were depicted in Fig. 7a. Although concentration$\phi$ decreases for higher levels of Lewis' number$Le$, it increases with larger variances in activation energy$E$. Fig. 7b illustrates the importance of the Marangoni number$Q$ and Marangoni ratio stricture$R$ on the concentration profile$\phi$. The concentration profile is decreased for the increasing estimations of $Q$and Marangoni ratio parameter$R$. The result of bioconvectionPeclet number and-Lewisamounton motile microbe's concentration is sketched in Fig. 8a. The rising variations of bioconvection Peclet quantity and Lewis amount lowered the motile bacteria profile. Fig. 8b reveals the importance$Q$ of the Marangoni ratio stricture for the profile of motile bacteria$\chi$. The motile microbe's profile's$\chi$ larger approximations$Q$ and$R$ decreases.

In this section, Tables 1–4 explores the numerical assessments of the limited Sherwood quantity$-\ \phi'(0)$, local microorganism density number$-\ \chi'(0)$, and local Nusselt amount$-\ \theta'(0)$ via modifications of the flow parameters. Table 1 lists the outcomes of the regional Nusselt number. Also, it should be noticed that the local Nusselt number decreases as the Prandtl number$Pr$ boots up. By increasing the mixed convection parameter's$\lambda$ fluctuations, local Sherwood number drops are explored in Table 2. Table 3 shows that for various Peclet number and bioconvection Lewis number evaluations, the local microorganism concentration numbers have increased. Table 4 determines the comparison of the attractive limitation determined for $f''(0)$ with that described by Ibrahim and Negera [47] and Sajid et al. [43] when all other flow parameters are set to zero. Here observed a good agreement between the published and current results.

## 5. Concluding remarks

The effects of Maxwell-Sutterby nanofluid flow motile microorganisms, activation energy, thermal conductivity, and bioconvection across such a stretched vertical sheet are studied here. The impacts of MHD and exponential heat sink/source are also depicted. The present study's key results are as follows:

- The speed outline changed when the magnetic restriction's value was greater, whereas it changed when the mixed convection parameter's value was higher.
- The temperature field is improved for higher differences in heat source parameter and heat sink parameter
- The thermal field decreased for greater values of the Prandtl number and increased for the thermal conductivity parameter.
- The concentration field is enhanced for the distinct values of the activation energy parameter while reducing the Brownian motion limitation.
- The microorganism field is reduced for the increasing trend Marangoni ratio parameter and Marangoni number.
- The present flow classical is used in various engineering problems, medical fields, cancer treatment, heat storage devices, and agriculture fields.

## Declaration of Competing Interest

The authors state that they have no known conflicting financial interests or personal ties that would appear to impugn the work described in this study.

## Data availability

The data that has been used is confidential.

## Acknowledgements

The authors would like to thank the Deanship of Scientific Research at Umm Al-Qura University for supporting this work by Grant Code: (22UQU4310392DSR27).

## References

[1] S.U.S. Choi, Enhancing thermal conductivity of fluids with nanoparticles, ASME Pub. Fed. 231 (1995) 99–106.
[2] J. Buongiorno, Convective transport in nanofuids, J. Heat Transf. 128 (2006) 240–250.
[3] K.L. Hsiao, Stagnation electrical MHD nanofluid mixed convection with slip boundary on a stretching sheet, Appl. Therm. Eng. 98 (2016) 850–861.
[4] M.M. Rashidi, N. Freidoonimehr, A. Hosseini, O.A. Beg, T.K. Hung, Homotopy simulation of nanofluid dynamics from a non-linearly stretching isothermal permeable sheet with transpiration, Meccanica 49 (2014) 469–482.
[5] M. Sheikholeslami, M.M. Bhatti, Forced convection of nanofluid in presence of constant magnetic field considering shape effects of nanoparticles, Int. J. Heat Mass Transf. 111 (2017) 1039–1049.
[6] M. Turkyilmazoglu, Condensation of laminar film over curved vertical walls using single and two-phase nanofluid models, Eur. J. Mech.-B/Fluids 65 (2017) 184–191.
[7] R. Ellahi, Recent Developments of Nanofluids, MDPI-Multidisciplinary Digital Publishing Institute, 2018.
[8] U. Farooq, H. Waqas, M.I. Khan, S.U. Khan, Y.M. Chu, S &Kadry, Thermally radioactive bioconvection flow of Carreau nanofluid with modified Cattaneo-Christov expressions and exponential space-based heat source, Alex. Eng. J. 60 (3) (2021) 3073–3086.
[9] M. Rashid, A. Alsaedi, T. Hayat, B. Ahmed, The magnetohydrodynamic flow of Maxwell nanofluid with binary chemical reaction and Arrhenius activation energy, Appl. Nanosci. (2019) 1–13.
[10] T. Tayebi, A.J &Chamkha, Magnetohydrodynamic natural convection heat transfer of a hybrid nanofluid in a square enclosure in the presence of a wavy circular conductive cylinder, J. Therm. Sci. Eng. Appl. 12 (3) (2020).
[11] T. Hayat, R. Riaz, A. Aziz, A &Alsaedi, Influence of Arrhenius activation energy in MHD flow of third-grade nanofluid over a nonlinear stretching surface with convective heat and mass conditions, Phys. A: Stat. Mech. Appl. (2020), 124006.
[12] T. Muhammad, H. Waqas, S.A. Khan, R. Ellahi, S.M &Sait, Significance of nonlinear thermal radiation in 3D Eyring–Powell nanofluid flow with Arrhenius activation energy, J. Therm. Anal. Calorim. (2020) 1–16.
[13] S.Z. Alamri, R. Ellahi, N. Shehzad, A. Zeeshan, Convective radiative plane Poiseuille flow of nanofluid through porous medium with slip: an application of Stefan blowing, J. Mol. Liq. 273 (2019) 292–304.
[14] I. Khan, A. Hussain, M.Y. Malik, S &Mukhtar, On magnetohydrodynamics Prandtl fluid flow in the presence of stratification and heat generation, Phys. A: Stat. Mech. Appl. 540 (2020), 123008.
[15] S.E. Awan, M.A.Z. Raja, A. Mehmood, S.A. Niazi, S &Siddiqa, Numerical treatments to analyze the nonlinear radiative heat transfer in MHD nanofluid flow with solar energy, Arab. J. Sci. Eng. (2020) 1–20.
[16] A. Gailitis, O. Lielausis, on the possibility to reduce the hydrodynamic resistance ofa plate in an electrolyte, Appl. Mag. Rep. Phy. Inst. 12 (1961) 143–146.
[17] A. Riaz, S.U. Khan, A. Zeeshan, S.U. Khan, M. Hassan, T Muhammad, Thermal analysis of the peristaltic flow of nanosized particles within a curved channel with second-order partial slip and porous medium, J. Therm. Anal. Calorim. 7 (2020) 1–3.
[18] M. Waqas, S. Jabeen, T. Hayat, S.A. Shehzad, A. Alsaedi, Numerical simulation for nonlinear radiated Eyring-Powell nanofluid considering magnetic dipole and activation energy, Int. Commun. Heat Mass Transf. 112 (2020), 104401.
[19] U. Farooq, H. Waqas, M.S. Aldhabani, N. Fatima, A. Alhushaybari, M.R. Ali, T Muhammad, Modeling and computational framework of radiative hybrid nanofluid configured by a stretching surface subject to entropy generation: using Keller box scheme, Arab. J. Chem. (2023), 104628.
[20] U. Farooq, H. Waqas, S.E. Alhazmi, A. Alhushaybari, M. Imran, R. Sadat, M.R Ali, Numerical treatment of casson nanofluid bioconvectional flow with heat transfer due to stretching cylinder/plate: variable physical properties, Arab. J. Chem. (2023), 104589.
[21] U. Farooq, H. Waqas, R. Makki, M.R. Ali, A. Alhushaybari, T. Muhammad, M. Imran, Computation of Cattaneo-Christov heat and mass flux model in Williamson nanofluid flow with bioconvection and thermal radiation through a vertical slender cylinder, Case Stud. Therm. Eng. (2023), 102736.
[22] W.A. Khan, Dynamics of gyrotactic microorganisms for modified Eyring Powell nanofluid flow with bioconvection and nonlinear radiation aspects, Waves Random Complex Media (2023) 1–11.
[23] P.P. Humane, V.S. Patil, M.D. Shamshuddin, G.R. Rajput, A.B. Patil, Role of bioconvection on the dynamics of chemically active Casson nanofluid flowing via an inclined porous stretching sheet with convective conditions, Int. J. Model. Simul. (2023) 1–20.
[24] S.A. Hussein, S.E. Ahmed, A.A &Arafa, Electrokinetic peristaltic bioconvective Jeffrey nanofluid flow with activation energy for binary chemical reaction, radiation, and variable fluid properties, ZAMM-J. Appl. Math. Mech./Z. tfürAngew. Math. Mech. 103 (1) (2023), e202200284.
[25] J. Iqbal, F.M. Abbasi, M. Alkinidri, H &Alahmadi, Heat and mass transfer analysis for MHD bioconvection peristaltic motion of Powell-Eyring nanofluid with variable thermal characteristics, Case Stud. Therm. Eng. (2023), 102692.

[26] E.U. Haq, S.U. Khan, T. Abbas, K. Smida, Q.M.U. Hassan, B. Ahmad, A.M. Galal, Numerical aspects of thermo-migrated radiative nanofluid flow towards a moving wedge with combined magnetic force and porous medium, Sci. Rep. 12 (1) (2022) 10120.

[27] Q. Ali, K. Al-Khaled, M.I. Khan, S.U. Khan, A. Raza, M. Oreijah, K &Guedri, Diffusion phenomenon for natural convection flow of classical Hartmann problem due to a cylindrical tube by generalized Fourier's theories: a Fractional analysis, Int. J. Mod. Phys. B (2022), 2350104.

[28] N.A. Qasem, A. Abderrahmane, S. Ahmed, O. Younis, K. Guedri, Z. Said, A &Mourad, Effect of a rotating cylinder on convective flow, heat, and entropy production of a 3D wavy enclosure filled by a phase change material, Appl. Therm. Eng. 214 (2022), 118818.

[29] M.A. Abbassi, R. Djebali, K &Guedri, Effects of heater dimensions on nanofluid natural convection in a heated incinerator-shaped cavity containing a heated block, J. Therm. Eng. 4 (3) (2018) 2018–2036.

[30] M.A. Abbassi, M.R. Safaei, R. Djebali, K. Guedri, B. Zeghmati, A.A &Alrashed, LBM simulation of free convection in a nanofluid-filled incinerator containing a hot block, Int. J. Mech. Sci. 144 (2018) 172–185.

[31] A.V. Kuznetsov, Thermo bioconvection in a suspension of oxytactic bacteria, Int. Commun. Heat Mass Transf. (2005) 991–999.

[32] Y. Li, H. Waqas, M. Imran, U. Farooq, F. Mallawi, I &Tlili, A numerical exploration of modified second-grade nanofluid with motile microorganisms, thermal radiation, and Wu's slip, Symmetry (Basel) 12 (3) (2020) 393.

[33] T. Muhammad, S.Z. Alamri, H. Waqas, D. Habib, R &Ellahi, Bioconvection flow of magnetized Carreau nanofluid under the influence of slip over a wedge with motile microorganisms, J. Therm. Anal. Calorim. (2020) 1–13.

[34] S.U. Khan, H. Waqas, M.M. Bhatti, M. Imran, Bioconvection in the rheology of magnetized couple stress nanofluid featuring activation energy and Wu's slip, J. Non-Equil. Thermodyn. 45 (1) (2020) 81–95.

[35] T. Zhang, S.U. Khan, M. Imran, I. Tlili, H. Waqas, N. Ali, Activation energy and thermal radiation aspects in bioconvection flow of rate-type nanoparticles configured by a stretching/shrinking disk, J. Energy Resour. Technol. (2020) 1–19.

[36] H. Waqas, M. Imran, T. Muhammad, S.M. Sait, R &Ellahi, Numerical investigation on bioconvection flow of OldroydB nanofluid with nonlinear thermal radiation and motile microorganisms over a rotating disk, J. Therm. Anal. Calorim. (2020).

[37] N.S. Khan, Q. Shah, A. Bhaumik, P. Kumam, P. Thounthong, I &Amiri, Entropy generation in bioconvection nanofluid flow between two stretchable rotating disks, Sci. Rep. 10 (1) (2020) 1–26.

[38] S.U. Mamatha, K.R. BABU, P.D. PRASAD, C.S.K. Raju, S.V.K &Varma, Mass transfer analysis of two-phase flow in a suspension of microorganisms, Arch. Thermodyn. (2020) 175–192.

[39] M. Ferdows, M.G. Reddy, F. Alzahrani, S. Sun, Heat and mass transfer in a viscous nanofluid containing a gyrotactic micro-organism over a stretching cylinder, Symmetry (Basel) 11 (9) (2019) 1131.

[40] N.A. Amirsom, M.J. Uddin, M.F.M. Basir, A. Ismail, O.A. Beg, A &Kadir, Three-dimensional bioconvection nanofluid flow from a bi-axial stretching sheet with anisotropic slip, SainsMalaysiana 48 (5) (2019) 1137–1149.

[41] S. Kasaragadda, I.M. Alarifi, M. Rahimi-Gorji, R &Asmatulu, Investigating the effects of surface superhydrophobicity on moisture ingression of nanofiber-reinforced bio-composite structures, Microsyst. Technol. 26 (2) (2020) 447–459.

[42] M.S. Ansari, O. Otegbeye, M. Trivedi, S.P &Gogo, Magnetohydrodynamic bio-convective Casson nanofluid flow: a numerical simulation by paired quasilinearisation, J. Appl. Comput. Mech. (2020).

[43] T. Sajid, S. Tanveer, Z. Sabir, J.L.G &Guirao, Impact of activation energy and temperature-dependent heat source/sink on Maxwell–Sutterby fluid, Math. Probl. Eng. 2020 (2020) 1–15.

[44] K.S. Nesamani, Estimation of automobile emissions and control strategies in India, Sci. Total Environ. 408 (8) (2010) 1800–1811.

[45] W.A. Khan, M. Ali, Recent developments in modeling and simulation of entropy generation for dissipative cross material with quartic autocatalysis, Appl. Phys. A 125 (2019) 1–9.

[46] J. Wang, W.A. Khan, Z. Asghar, M. Waqas, M. Ali, M. Irfan, Entropy-optimized stretching flow based on non-Newtonian radiative nano liquid under binary chemical reaction, Comput. Methods Prog. Biomed. 188 (2020), 105274.

[47] W. Ibrahim, M &Negera, MHD slip flow of upper-convected Maxwell nanofluid over a stretching sheet with chemical reaction, J. Egypt. Math. Soc. 28 (1) (2020) 7.